Journal of South American Earth Sciences 42 (2013) 144–149

Contents lists available at SciVerse ScienceDirect

Journal of South American Earth Sciences

journal homepage: www.elsevier.com/locate/jsames

Crustal-scale electrical conductivity anomaly beneath inflating Lazufre volcanic complex, Central Andes

Ingmar Budach [a], Heinrich Brasse [a,*], Daniel Díaz [b]

[a] Freie Universität Berlin, Fachrichtung Geophysik Malteserstr. 74-100, 12249 Berlin, Germany
[b] Departamento de Geofísica, Universidad de Chile, Blanco Encalada 2002, Santiago, Chile

ARTICLE INFO

Article history:
Received 3 September 2012
Accepted 15 November 2012

Keywords:
Magnetotellurics
Central Andes
Volcanoes
Surface deformation

ABSTRACT

Large-scale surface deformation was observed at Lazufre volcanic center in the Central Andes of Northern Chile/Northwestern Argentina by means of Interferometric Synthetic Aperture Radar (InSAR). Uplift started there after 1998 and increased dramatically in the following years up to a rate of 3 cm/a. Lazufre is now one of the largest deforming volcano systems on Earth, but the cause for uplift – likely influx of magmatic material into the crust – is still poorly understood.

In the beginning of 2010 a magnetotelluric survey was conducted to delineate the electrical conductivity distribution in the area. Several long-period magnetotelluric (LMT) sites and two broadband magnetotelluric (BBMT) sites were set up on an EW trending profile crossing the volcanic center; furthermore some LMT sites were arranged circularly around Lazufre complex and adjacent Lastarria volcano. Data were processed using an algorithm for robust and remote reference transfer function estimation. Electrical strike directions were estimated and induction arrows were derived. Although electrical strike is rather ambiguous, in a first step a 2-D resistivity model was calculated. The most prominent feature of this model is a well conducting structure rising from the upper mantle to the shallow crust beneath the center of elevation. This can be interpreted as partial melts ascending from the asthenospheric wedge and feeding a potential magma reservoir beneath Lazufre volcanic center. An improved model is finally achieved by 3-D inversion, supporting this feature. We assume that these rising melts are the source of the observed uplift at Lazufre complex.

1. Introduction

Insights into the spatio-temporal development of volcanic centers have recently become available by images of Satellite Interferometric Synthetic Aperture Radar (InSAR). Pritchard and Simons (2002) created radar interferograms for about 900 of the approximately 1100 volcanic edifices in the Central Andes. Active deformation at four circular-elliptical volcanic centers was observed. In this work we focus on the area in the vicinity of the volcanoes Lastarria and Cordón del Azufre, which is often termed "Lazufre", an acronym of Lastarria and Azufre (Pritchard and Simons, 2002).

The Lazufre volcanic complex is situated in the Western Cordillera of the Central Andes, the location of the present magmatic arc, at approximately 25.1°S on the border between Argentina and Chile (Fig. 1). The magmatic arc has developed due to subduction of the Nazca plate beneath the South American plate and has migrated 200 km eastwards since 120 Ma (Scheuber et al., 2006). Eruptions of caldera complexes resulted in immense Late Miocene to Pliocene ignimbrite deposits in the magmatic arc and the southern end of the Altiplano plateau (Altiplano-Puna Volcanic Complex) covering an area of about 50,000 km^2 (de Silva, 1989). For an overview of spatial and temporal plateau development see, e.g., Allmendinger et al. (1997).

Surprisingly, the center of surface deformation at Lazufre is not associated with any known volcanic edifice, but lying between Lastarria and Cordón del Azufre volcanoes (cf. ellipse in 1). Both volcanic edifices are considered to be "potentially active". While no historical activity has been recorded at Cordón del Azufre, Lastarria shows persistent fumarolic activity (de Silva and Francis, 1991). The activity at Lastarria is thought to move to the north (Naranjo and Francis, 1987), although deformation has been observed to the south (Pritchard and Simons, 2004a). In later InSAR measurements a clear uplift signal is visible at Lastarria (Fig. 1, Ruch et al. (2009)). Surface elevation at Lazufre volcanic complex is time-depending: While no deformation was observed in the interferograms before

* Corresponding author.
E-mail address: heinrich.brasse@fu-berlin.de (H. Brasse).

0895-9811/$ – see front matter © 2012 Elsevier Ltd. All rights reserved.
http://dx.doi.org/10.1016/j.jsames.2012.11.002

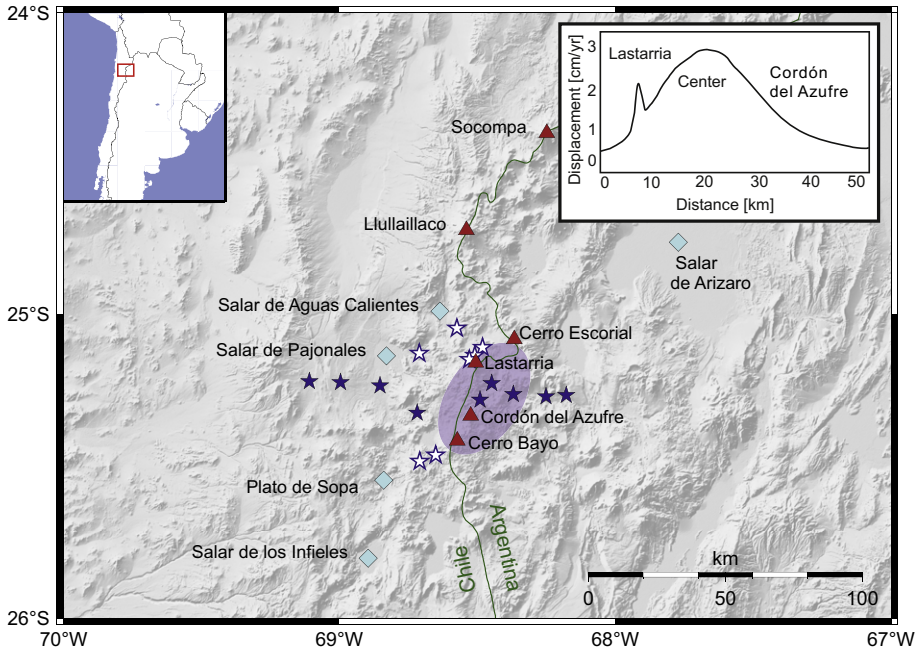

Fig. 1. SRTM-based shaded relief map of the study zone and location of MT sites in the Central Andes, Northern Chile/Northwestern Argentina. Blue stars indicate those sites which were used for 2-D modeling. Blue framed stars indicate stations, which were arranged circularly around Lazufre volcanic complex. Red triangles mark prominent volcanic edifices; maximal uplift occurs between Lastarria and Cordón de Azufre volcanoes. Transparent ellipse indicates center of surface deformation after Ruch and Walter (2010) and isoline of surface deformation in the upper right corner is redrawn after Ruch et al. (2009). (For interpretation of the references to colour in this figure legend, the reader is referred to the web version of this article.)

1998, there was a clear signal in three interferograms afterwards. Uplift at Lazufre increased drastically up to a rate of about 3 cm/a (cf. isoline of surface deformation for a N–S profile in Fig. 1) and a spatial extent of 1800 km^2, with a long axis up to 50 km (Ruch et al., 2009). It is now one of the largest deforming volcano systems on earth, comparable in size with Yellowstone and Long Valley (both USA) and could represent an evolving pre-caldera silicic system (Froger et al., 2007). Two possible scenarios explaining the inflation were hypothesized: It could either be a new intrusion of a sill expanding laterally at depth or a pre-existing magma chamber inflating at depth (Ruch et al., 2008). For a broader discussion on possible sources of deformations at volcanic complexes see for example Zurek et al. (2012).

Hydrothermal fluids and partial melts of volcanic systems are characterized by high electrical conductivity and therefore a good target for geophysical methods sensitive to conductivity, in particular for magnetotellurics (e.g., Brasse and Eydam (2008); Aizawa et al. (2005)). Natural geomagnetic variations – which are caused by variations of the solar wind for periods $T > 1$ s – induce electrical currents in the conductive earth which in turn give rise to a secondary magnetic field. A scale length is provided by the skin depth $\delta \approx 0.5\rho T$, with resistivity ρ. From the impedance, the principal transfer function is determined from the ratio of horizontal electric and magnetic fields, apparent resistivities and phases are calculated. Another transfer function is the tipper, the ratio of vertical to horizontal magnetic fields; from this so-called induction arrows or vectors are calculated which are indicative of lateral conductivity contrasts.

Previous long-period magnetotelluric measurements were conducted in the Central Andes by Brasse et al. (2002) and Brasse and Eydam (2008) along several transects crossing the magmatic arc and the Altiplano high plateau. Beneath the southern Altiplano at 21°S, a large high-conductivity zone in the mid-deep crust was interpreted as partial melts and fluids. It prohibits the resolution of upper mantle structures. Farther to the north at 17°S this conductor is missing; instead, an anomaly is modeled in the asthenosphere which is thought to originate from dehydration of the subducting Nazca slab. Although this interpretation is in agreement with the standard subduction model, the conductor is offset by almost 100 km from the volcanic arc. Notably, no enhanced conductivity was detected beneath the volcanoes themselves.

The high-conductivity zone in the backarc crust beneath the Altiplano is thought to extend farther south into the Puna, as was shown by Díaz et al. (2012). Again, this study found no evidence for enhanced conductivity beneath the volcanic arc. This is perhaps a hint at an emerging shift of the magmatic system in the Central Andes towards the east.

2. Data evaluation and strike directions

During a field campaign in January/February 2010 a magnetotelluric experiment was conducted in the Central Andes of Northern Chile and Northwestern Argentina. As part of this experiment 12 long period magnetotelluric (LMT) and two broadband magnetotelluric (BBMT) stations were arranged at the Lazufre volcanic complex. The other part of the experiment was centered around Lascar volcano farther north and is described in Díaz et al. (2012). Seven of the LMT stations and the two AMT stations were arranged along an approximately 100 km long EW trending profile at 25.1°S latitude, crossing the Western Cordillera with the present magmatic arc. The other stations were set circularly around the Lazufre volcanic complex (cf. Fig. 1). The LMT instruments cover a period range between $T = 10$ s–10,000 s and the BBMT a period range between $T = 0.005$ s–1000 s, respectively.

Unfortunately, due to serious logistical difficulties in the beginning of the field campaign not as many stations as originally planned could be installed. Hence there is a lack in station coverage, especially in the eastern part of the measuring area. Moreover, Lazufre is a remote region in the High Andes and many parts of the study area are difficult to access by car. This complicates the

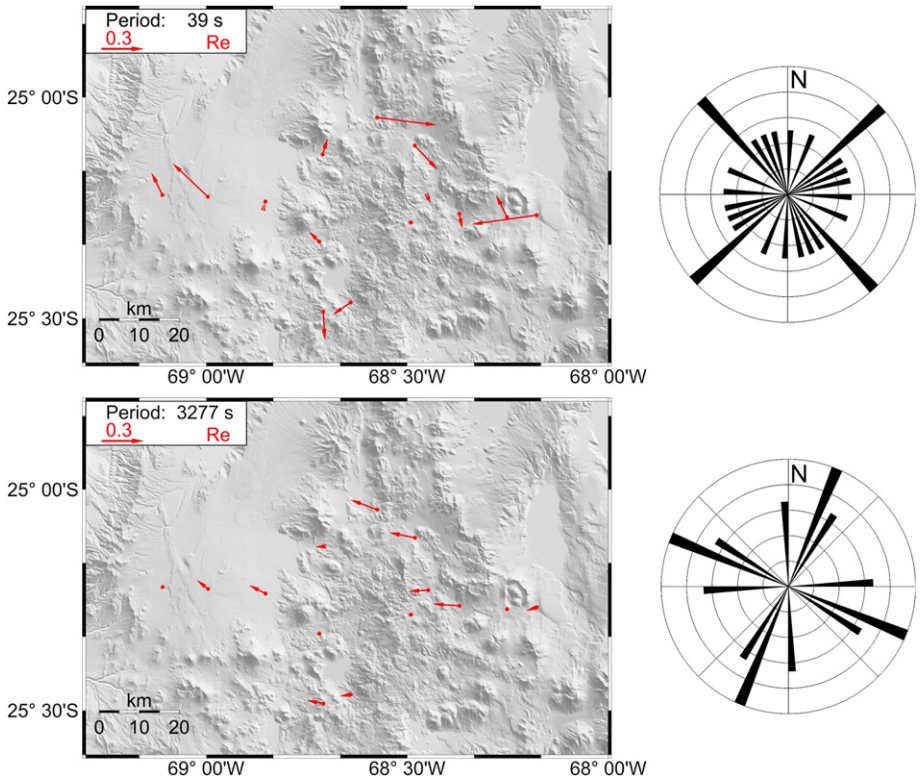

Fig. 2. Left: Map of the Lazufre volcanic complex with real induction arrows in Wiese convention. The behavior at short periods (39 s, top left) is mainly due to the distribution of well-conducting salars (salt pans) at the surface. For long periods (3277 s, bottom left) induction vectors indicate a good conductor west of the profile. Note that red dots indicate stations where bad data were excluded. Right: Electrical strike directions calculated after Smith (1995) for the period range 10 s–100 s (above) and 1000 s–10 000 s (below). (For interpretation of the references to colour in this figure legend, the reader is referred to the web version of this article.)

locating of places for station setup, particularly in the center of surface deformation. A further aggravating factor was an exceptionally low solar activity during the time of the field campaign, leading to lower signal-to-noise ratio than usual. However, by applying remote reference and robust techniques for data processing (Egbert and Booker, 1986) an acceptable quality of transfer functions could be achieved (see examples later in Fig. 5 in the 3-D section).

Electrical strike directions from impedances were calculated using the multi-site, multi-frequency algorithm of Smith (1995), resulting in ambiguous directions for different periods, i.e., it's difficult to assign a single best strike for all sites and periods (cf. Fig. 2). Another option to infer electrical strike is to analyze induction arrows which are calculated from the tipper, the ratio of vertical to horizontal magnetic fields. They are plotted according to the convention of Wiese (1962), i.e., real parts of induction vectors point away from well conducting structures in a 2-D setting (Fig. 2). Similar to the impedance strike directions, they show an ambiguous behavior for short periods. They are aligned towards a northwest direction for intermediate periods and show influences of coastal effects for periods near 10,000 s. The chaotic behavior at short periods is probably caused by the presence of numerous salars (salt pans) in that region, internally drained basins filled with highly conductive brines (see section below).

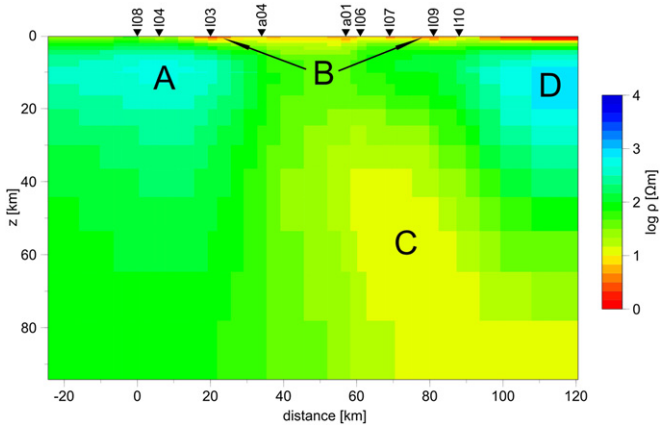

Fig. 3. 2-D model of the Lazufre volcanic complex. The most prominent feature is a well conducting structure ascending from the upper mantle. RMS for this model is 2.18.

Keeping the ambiguous strike directions in mind, two-dimensional modeling of this data set can only be of preliminary character and preparatory for later three-dimensional modeling. By taking the directions of the induction vectors and the impedance strike directions into account, a common electrical strike direction of approximately N25°E for the complete period range was estimated (Budach, 2011) and used for the 2-D inversion described in the next section. This angle corresponds roughly to the major axis of the elliptical surface deformation (cf. Fig. 1).

3. Two-dimensional model

A 2-D model was calculated by employing the non-linear conjugate gradient algorithm of Rodi and Mackie (2001). As usual, a number of tests regarding smoothing parameters, starting models, error floors etc. were conducted. For the "final" model, all components, i.e., TE mode (tangential-electric, electric field parallel to strike), TM mode (tangential-magnetic, magnetic field parallel to

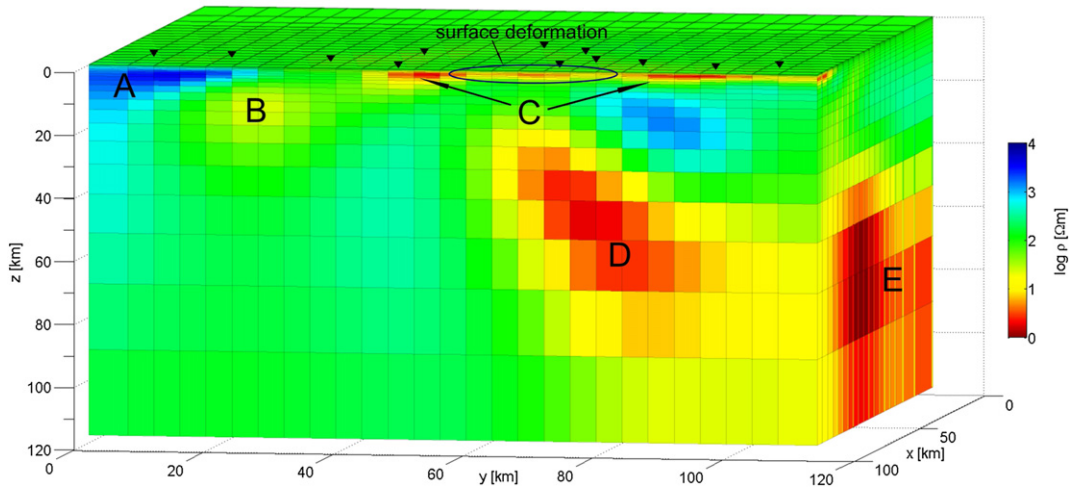

Fig. 4. 3-D model of Lazufre volcanic complex showing the same prominent features like the 2-D model. The major finding is a highly conductive body beneath the center of surface elevation at Lazufre (marked as D). RMS for this model is 1.45. Note that the color scale is slightly different from the 2-D model (Fig. 3). Moho depth estimates vary between 60 and 65 km according to Wölbern et al. (2009) and Heit et al. (2007).

strike) and tipper were used for the inversion. The regularization factor was set to $\tau = 10$ and error floors to 20% for apparent resistivities and 5% for phases in order to minimize static shift problems by assigning a higher weight to phases. A starting model was used with a homogenous half-space (resistivity 100 Ωm), the Pacific Ocean (0.3 Ωm, with crude bathymetry) and the subducting Nazca plate (1000 Ωm and using contours for the subducting slab after Cahill and Isacks (1992)). Topographic effects are small at long periods ($T > 10$ s) and were thus neglected. The inversion was performed with 200 iterations without extra inversion for static shift and then 50 additional iterations with inversion for static shift enabled. The best fitting model achieved an RMS of 2.18 (Budach, 2011).

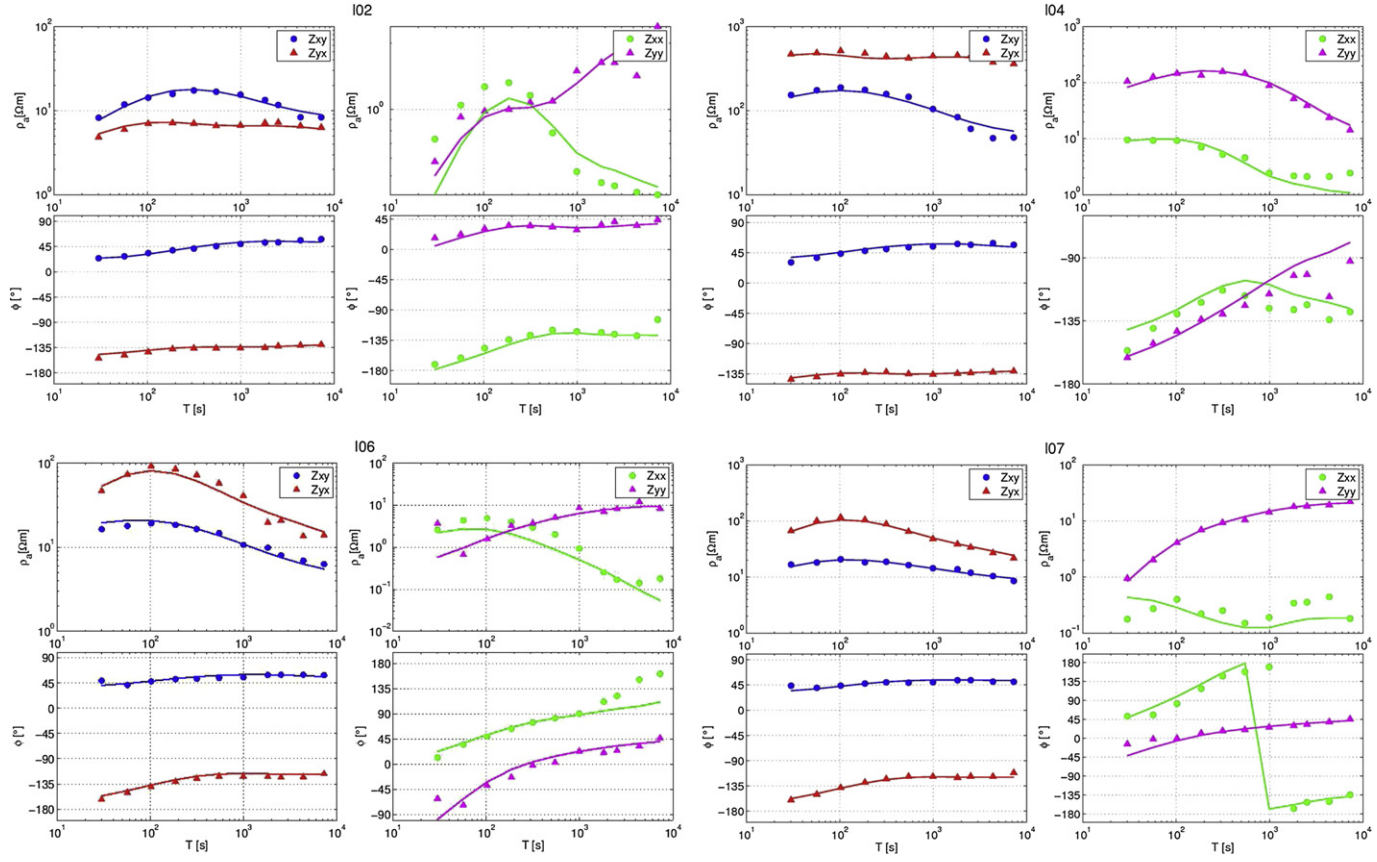

Fig. 5. Comparison between measured data (dots) and model response (continuous lines) at four sites is shown. Minor diagonals are drawn in red and blue, major diagonals in green and purple. Site l04 is in the Precordillera in the western part of the profile, l02 in the center of the profile and l06 and l07 are in the eastern part of the profile in Argentina. (For interpretation of the references to colour in this figure legend, the reader is referred to the web version of this article.)

A highly resistive block is resolved beneath sites l08 and l04 at the western margin of the profile (marked as A in Fig. 3). This can be interpreted as a Late Cretaceous plutonic intrusion, which has also been observed at the southern part of the Salar de Atacama basin (Díaz et al., 2012) and SW of the Salar de Atacama (Oncken et al., 2006).

In the center of the profile several well conducting structures (marked as B and associated arrows in Fig. 3) are observed. They are resolved at the surface down to shallow depths and show resistivities of a few Ωm. In the investigation area, as well as in other parts of the Central Andes, numerous salars (salt pans) are found (Allmendinger et al., 1997). These are internally drained basins filled with evaporites and often highly-conductive brines, which can reach thicknesses of several hundred meters.

The most striking and most important feature of this model is a well conducting structure marked as C in Fig. 3. It rises from the upper mantle towards the shallow crust and shows a resistivity of around 10 Ωm with increasing resistivity towards the shallow crust (some tens of Ωm). Note that an average depth to the Moho of about 60–65 km is determined for this region (Wölbern et al., 2009). This feature appears in all tested models, with slightly different shapes. However, the rise from the upper mantle and the pathway towards shallow depths were observed in each model. Taking these arguments into account we assume this structure to be an image of partial melts rising from the upper mantle and feeding an intracrustal magma reservoir. These rising melts are likely to be the source of surface deformation at Lazufre.

Another highly resistive feature is seen east of the profile at midcrustal depths with a resistivity of approximately 1000 Ωm (marked as D in Fig. 3). Interpretation of this structure is somewhat doubtful, since it lies outside the profile and, generally, model fit is worse at the eastern part of the profile.

4. Three-dimensional inversion of Lazufre data

In a second step, a 3-D inversion was performed applying the 3-D code of Siripunvaraporn et al. (2005a). This program is an extension of the 2-D data space Occam's inversion (Siripunvaraporn and Egbert, 2000) and inverts the eight components of the impedance tensor. In order to reduce computational time, the algorithm uses the data space method, where all computations depend on the size of data N, not the size of model parameters M. Since the general case for MT data is $N << M$, the computational efficiency can be increased significantly and thus makes it practical to be used on standard PCs. A subset of data was chosen, eliminating data points of poor quality and selecting 4 periods per decade. Hence the size of the data N and thus memory size and computational time are limited to reasonable values.

The model was discretized into 49 cells in N–S and E–W direction, spanning an area of 3200 km in each direction, and 31 cells in z-direction up to a depth of 560 km. The cell size in the center of the grid was set to 4×4 km. A homogeneous 100 Ωm-halfspace and the Pacific Ocean with crude bathymetry and 0.3 Ωm resistivity was used as a starting model. All sites marked in Fig. 1 were used, including the two broadband sites, but restricting the period range to $T > 10$ s. As for the 2-D inversion topography was neglected due to the long period range used in this experiment. After 9 iterations a best fitting model with an RMS of 1.45 was achieved (cf. Fig. 4 for inversion result and Fig. 5 for data fit). Although the 3-D inversion yields in many aspects similar results as the 2-D inversion, significant differences are observed as well and discussed below. Data fit is generally good, not only for the minor diagonal, but also for the major diagonal.

Beneath the westernmost sites, a resistive block similar to the 2-D model is resolved (marked as A in Figs. 3 and 4). It is located beneath the Chilean Precordillera and could be, as discussed above, an image of a Late Cretaceous plutonic intrusion (cf. Díaz et al. (2012); Oncken et al. (2006)).

Different from the 2-D model, a highly conductive body is observed at relatively shallow crustal depths in the western part of the profile (B in Fig. 4) beneath the Precordillera. In a previous MT study farther to the north, a similar conductivity anomaly was also imaged in the crust of the Chilean forearc (Brasse et al., 2002). We thus conclude that the newly found conductor is also connected to the Precordillera Fault System (PFS), a mega shear zone extending over 1000 km in the Chilean forearc (Reutter et al., 1991). A detailed magnetotelluric study north of Chuquicamata copper mine revealed the near-surface structure of the PFS as highly conductive (Hoffmann-Rothe et al., 2004). In addition, this is the location where the trace of the Culumpaja lineament – one of a series of lineaments running obliquely through the Central Andes at this latitude (Riller et al., 2001; Richards and Villeneuve, 2002) – crosses the PFS which may further enhance conductivity.

Furthermore and as in the 2-D inversion result some salars are imaged at shallow depths (C in Fig. 4). Of course, the true dimension of these salars is not resolved due to lack of sites.

The most striking feature of this model is a highly conductive structure marked as D in Fig. 4. It shows a similar shape and a slightly higher conductivity as in the 2-D model. This is somewhat remarkable as it contradicts a frequent observation, namely that conductivity is enhanced if 3-D data are interpreted in a 2-D manner (see, e.g., Siripunvaraporn et al. (2005b)). Note that in the 3-D case, this well conducting structure appears to rise from a southeastern direction towards the center of the profile. Taking the results of the 2-D and 3-D inversion into account, we interpret this high-conductivity zone as an image of partial melts ascending from upper mantle depths towards the shallow crusts. Assuming a two-phase system and applying the Hashin-Shtrikman upper bound (which means full connectivity of the fluid phase) with a melt resistivity of 0.2–0.1 Ωm, a melt ratio of 5–8 vol% can be estimated. We assume these partial melts to be the major cause for uplift at the Lazufre volcanic complex.

At the eastern margin of the 3-D model a vast high-conductivity zone is resolved at deep crustal and upper mantle depths. It is possible that this is an image of the same highly conductive zone as described in earlier magnetotelluric studies in the Central Andes (Brasse et al., 2002; Brasse and Eydam, 2008; Díaz et al., 2012). This observation would support the hypothesis of Brasse and Eydam (2008) of an emerging shift of the magmatic system in the Central Andes. Due to the lack of sites in Argentina, however, this structure is not well resolved and clearly requires more measurements in the Puna.

Some sensitivity test were carried out in order to constrain the existence of two anomalies: the good conductor beneath the Precordillera (B in Fig. 4) and the depth extent of the high conductivity zone beneath the center of surface deformation (D in Fig. 4), in particular its connection to the upper mantle. Both structures have been substituted by cells of 100 Ωm and inversion was started over again. Since well conducting structures with a similar shape reappeared and the model's RMS did not change significantly, both anomalies appear to be valid.

5. Conclusions

2-D and 3-D inversions of long-period and broadband magnetotelluric data image a well conducting anomaly beneath the Lazufre volcanic complex. It ascends from the upper mantle towards the upper crust with resistivities as low as a few Ωm till some tens of Ωm. This structure is recovered in all tested models, in 2-D as

well as in 3-D inversions. The orientation of induction vectors supports this feature.

The spatial extent of this feature is in good agreement with surface deformation detected at the Lazufre volcanic complex (Pritchard and Simons, 2002, 2004a,b; Ruch et al., 2008, 2009; Ruch and Walter, 2010). Therefore we suggest that a major cause of uplift at Lazufre is due to partial melts ascending from depth and feeding an intracrustal magma reservoir. It would be of particular interest in a future campaign to conduct more measurements towards the east on the Puna in order to account for the eastern extension of the good conductor beneath Lazufre.

Another important feature resolved in this study is a high conductivity zone beneath the Puna high plateau at the eastern margin of the profile (E in Fig. 4). This is in good agreement with previous magnetotelluric studies conducted in the Central Andes (Brasse et al., 2002; Brasse and Eydam, 2008; Díaz et al., 2012) and seismic attenuation tomography (Schurr et al., 2003). One could therefore argue that this high conductivity zone is common to almost the entire southern Altiplano-Puna high plateau.

Acknowledgments

We are grateful to Hans Wilke and Guillermo Chong (Universidad Católica del Norte, Antofagasta) as well as Cristina Pomposiello and Alicia Favetto (Universidad de Buenos Aires) and the German Embassy in Buenos Aires for logistical support. Thomas Walter provided us with essential information about the location. Thanks to Dana Weichelt, Faustino Ticona and the Chilean students who helped us during the field campaign in 2010. The 3-D inversion code was provided by Weerachai Siripunvaraporn. Most of the plots were prepared using the GMT package of Wessel and Smith (1998). This work has been funded by German Science Foundation (DFG), grant BR 1351/5-2.

Appendix A. Supplementary data

Supplementary data related to this article can be found at http://dx.doi.org/10.1016/j.jsames.2012.11.002.

References

Aizawa, K., Yoshimura, R., Oshiman, N., Yamazaki, K., Uto, T., Ogawa, Y., Tank, S.B., Kanda, W., Sakanaka, S., Furukawa, Y., Hashimoto, T., Uyeshima, M., Ogawa, T., Shiozaki, I., Hurst, A.W., 2005. Hydrothermal system beneath Mt. Fuji volcano inferred from magnetotellurics and electric self-potential. Earth Planet. Sci. Lett. 235, 343–355. http://dx.doi.org/10.1016/j.epsl.2005.03.023.

Allmendinger, R.W., Jordan, T.E., Kay, S.M., Isacks, B.L., 1997. The evolution of the Altiplano-Puna plateau of the Central Andes. Ann. Rev. Earth Planet. Sci. 25, 139–174.

Brasse, H., Lezaeta, P., Rath, V., Schwalenberg, K., Soyer, W., Haak, V., 2002. The Bolivian Altiplano conductivity anomaly. J. Geophys. Res. 107 (B5). http://dx.doi.org/10.1029/2001JB000391

Brasse, H., Eydam, D., 2008. Electrical conductivity beneath the Bolivian Orocline and its relation to subduction processes at the South American continental margin. J. Geophys. Res. 113, B07109. http://dx.doi.org/10.1029/2007JB005142.

Budach, I., 2011. Preliminary 2D inversion of the Lazufre volcanic area in the Central Andes, Northern Chile. B.Sc. thesis, Fachrichtung Geophysik, FU Berlin.

Cahill, T., Isacks, B., 1992. Seismicity and shape of the Subducted Nazca plate. J. Geophys. Res. 97 (B12), 17503–17529. http://dx.doi.org/10.1029/92JB00493.

de Silva, S.L., 1989. Altiplano-Puna volcanic complex of the Central Andes. Geology 17, 1102–1106.

de Silva, S.L., Francis, P.W., 1991. Volcanoes of the Central Andes. Springer-Verlag, New York.

Díaz, D., Brasse, H., Ticona, F., 2012. Conductivity distribution beneath Lascar volcano (Northern Chile) and the Puna, inferred from magnetotelluric data. J. Volc. Geotherm. Res., 217–218. http://dx.doi.org/10.1016/j.jvolgeores.2011.12.007.

Egbert, G.D., Booker, J.R., 1986. Robust estimation of geomagnetic transfer functions. Geophys. J.R. Astr. Soc. 87, 173–194.

Froger, J.-L., Remy, D., Bonvalot, S., Legrand, D., 2007. Two scales of inflation at Lastarria-Cordon del Azufre volcanic complex, central Andes, revealed from ASAR-ENVISAT interferometric data. Earth Planet. Sci. Lett. 255 (1–2), 148–163. http://dx.doi.org/10.1016/j.epsl.2006.12.012.

Heit, B., Sodoudi, F., Yuan, X., Bianchi, M., Kind, R., 2007. An S receiver function analysis of the lithospheric structure in South America. Geophys. Res. Lett. 34. 0.1029/2007GL030317.

Hoffmann-Rothe, A., Ritter, O., Janssen, C., 2004. Correlation of electrical conductivity and structural damage at a major strike-slip fault in northern Chile. J. Geophys. Res. 109. http://dx.doi.org/10.1029/2004JB003030

Naranjo, J.A., Francis, O., 1987. High velocity debris avalanche at Lastarria volcano in the north Chilean Andes. Bull. Volc. 49, 509–514.

Oncken, O., Hindle, D., Kley, J., Elger, K., Victor, P., Schemmann, K., 2006. Deformation of the Central Andean upper plate system – facts, fiction, and constraints for plateau models. In: Oncken, O., et al. (Eds.), The Andes: Active Subduction Orogeny. Frontiers in Earth Sciences. Springer, Berlin, pp. 3–27.

Pritchard, M.E., Simons, M., 2002. A satellite geodetic survey of large-scale deformation of volcanic centers in the Central Andes. Nature 418. http://dx.doi.org/10.1038/nature00872.

Pritchard, M.E., Simons, M., 2004a. An InSAR-based survey of volcanic deformation in the central Andes. Geochem. Geophys. Geosyst. 5, Q02002. http://dx.doi.org/10.1029/2003GC000610.

Pritchard, M.E., Simons, M., 2004b. Surveying volcanic arcs with satellite radar interferometry: the central Andes, Kamchatka and beyond. GSA Today 14 (8). http://dx.doi.org/10.1130/1052-5173(2004)014<4:SVAWSR>2.0.CO;2.

Reutter, K.J., Scheuber, E., Helmcke, D., 1991. Structural evidence of orogen-parallel strike-slip displacements in the Precordillera of northern Chile. Geol. Rdsch. 80, 135–153.

Richards, J.P., Villeneuve, M., 2002. Characteristics of late Cenozoic volcanism along the Archibarca lineament from Cerro Llullaillaco to Corrida de Cori, northwest Argentina. J. Volc. Geotherm. Res. 116 (3), 161–200.

Riller, U., Petrinovic, I., Ramelow, J., Strecker, M., Oncken, O., 2001. Late Cenozoic tectonism, collapse caldera and plateau formation in the central Andes. Earth Planet. Sci. Lett. 188, 299–311.

Rodi, W., Mackie, R.L., 2001. Nonlinear conjugate gradients algorithm for 2-D magnetotelluric inversions. Geophysics 66, 174–187.

Ruch, J., Anderssohn, J., Walter, T.R., Motagh, M., 2008. Caldera-scale inflation of the Lazufre volcanic area, south America: evidence from InSAR. J. Volc. Geotherm. Res. 174. http://dx.doi.org/10.1016/j.jvolgeores.2008.03.009

Ruch, J., Manconi, A., Zeni, G., Solaro, G., Pepe, A., Shirzaei, M., 2009. Stress transfer in the Lazufre volcanic area, central Andes. Geophys. Res. Lett. 36. http://dx.doi.org/10.1029/2009GL041276

Ruch, J., Walter, T.R., 2010. Relationship between the InSAR-measured uplift, the structural framework, and the present-day stress field at Lazufre volcanic area, central Andes. Tectonophysics 492. http://dx.doi.org/10.1016/j.tecto.2010.06.003.

Scheuber, E., Mertmann, D., Harald, E., Silva-Gonzalez, P., Heubeck, C., Reutter, K.J., Jacobshagen, V., 2006. Exhumation and basin development related to formation of the central Andean plateau, 21°S. In: Oncken, O., et al. (Eds.), The Andes: Active Subduction Orogeny. Frontiers in Earth Sciences. Springer, Berlin, pp. 285–301.

Schurr, B., Asch, G., Rietbrock, A., Trumbull, R., Haberland, C., 2003. Complex patterns of fluid and melt transport in the central Andean subduction zone revealed by attenuation tomography. Earth Planet. Sci. Lett. 215. http://dx.doi.org/10.1016/S0012-821X(03)00441-2

Siripunvaraporn, W., Egbert, G., 2000. An efficient data-subspace inversion method for 2-D magnetotelluric data. Geophysics 65, 791–803.

Siripunvaraporn, W., Egbert, G., Lenbury, Y., Uyeshima, M., 2005a. Three-dimensional magnetotelluric inversion: data-space method. Phys. Earth Planet. Inter. 150, 3–14.

Siripunvaraporn, W., Egbert, G., Uyeshima, M., 2005b. Interpretation of two-dimensional magnetotelluric profile data with three-dimensional inversion: synthetic examples. Geophys. J. Int. 160, 804–814.

Smith, J.T., 1995. Understanding telluric distortion matrices. Geophys. J. Int. 122, 219–226.

Wessel, P., Smith, W.H.F., 1998. New, improved version of the generic mapping tools released. EOS Trans. AGU 79, 579.

Wiese, H., 1962. Geomagnetische Tiefentellurik Teil II: die Streichrichtung der Untergrundstrukturen des elektrischen Widerstandes, erschlossen aus geomagnetischen Variationen. Pure App. Geophys. 52, 83–103.

Wölbern, I., Heit, B., Yuan, X., Asch, G., Kind, R., Tawackoli, S., Wilke, H., 2009. Receiver function images from the Moho and the slab beneath the Altiplano and Puna plateaus in the Central Andes. Geophys. J. Int. 177, 296–308.

Zurek, J., William-Jones, G., Johnson, D., Eggers, A., 2012. Constraining volcanic inflation at Three Sisters volcanic field in Oregon, USA, through microgravity and deformation modeling. Geochem. Geophys. Geosyst. 13, Q10013. http://dx.doi.org/10.1029/2012GC004341.